

Dark matter signals from timing spectra at neutrino experiments

Bhaskar Dutta^{a*}, Doojin Kim^{b†}, Shu Liao^{a‡}, Jong-Chul

Park^{c§}, Seodong Shin^{d¶}, and Louis E. Strigari^{a**}

^a *Mitchell Institute for Fundamental Physics and Astronomy,*

Department of Physics and Astronomy,

Texas A&M University, College Station, TX 77843, USA

^b *Department of Physics, University of Arizona, Tucson, AZ 85721, USA*

^c *Department of Physics, Chungnam National University, Daejeon 34134, Republic of Korea*

^d *Department of Physics & IPAP, Yonsei University, Seoul 03722, Republic of Korea*

Abstract

We propose a *novel* strategy to search for new physics in timing spectra, envisioning the situation in which a new particle comes from the decay of its heavier partner with a finite particle width. The timing distribution of events induced by the dark matter particle scattering at the detector may populate in a relatively narrow range, forming a “resonance-like” shape. Due to this structural feature, the signal may be isolated from the backgrounds, in particular when the backgrounds are uniformly distributed in energy and time. For proof of the principle, we investigate the discovery potential for dark matter from the decay of a dark photon in the COHERENT experiment, and show the exciting prospects for exploring the associated parameter space with this experiment. We analyze the existing CsI detector data with a timing cut and an energy cut, and find, for the first time, an excess in the timing distribution which can be explained by such dark matter. We compare the sensitivity to the kinetic mixing parameter (ϵ) for current and future COHERENT experiments with the projected limits from LDMX and DUNE.

* E-mail address: dutta@physics.tamu.edu

† E-mail address: doojinkim@email.arizona.edu

‡ E-mail address: ikaros@physics.tamu.edu

§ E-mail address: jcpark@cnu.ac.kr

¶ E-mail address: seodongshin@yonsei.ac.kr

** E-mail address: strigari@tamu.edu

I. INTRODUCTION

Numerous theoretical and experimental ideas have been put forth to identify the mass and associated interactions of dark matter (DM) particles. Since the Standard Model (SM) does not contain DM and traditional WIMP-based searches have not yet detected DM [1], expanding the search of parameter space is well-justified [2]. Many models of light DM (\lesssim GeV) emerge from a hidden/visible sector where light mediators (e.g., a dark photon) interact with DM [3–8]. Because the DM mass is light in these models, it is difficult to detect such DM in traditional WIMP-based direct detection experiments.

In this paper we develop a *novel* strategy to search for light DM which couples with light mediators, using data from the ongoing COHERENT experiment [9]. COHERENT makes use of a proton beam which impinges on a Hg target at the Spallation Neutron Source (SNS). Among the pions that are produced, π^+ decays create prompt muon neutrinos and delayed anti-muon and electron neutrinos. The measured energy spectra have been used to investigate new physics associated with neutrino non-standard interactions (NSI) [10, 11] due to heavy or light mediators [12–19], generalized scalar and vector neutrino interactions [20], hidden sector models [21], and sterile neutrinos [22, 23]. It also sets independent constraints on the effective neutron size distribution of CsI [24–26]. Since the proton beam is pulsed, the measured timing spectra may be used to distinguish between prompt and delayed events. The combined timing and energy spectra have been utilized to understand new physics models with neutrino flavor-dependent NSI [27].

We show how both the timing and energy data from the COHERENT experiment can be used to search for light, $\lesssim 1$ GeV, DM. For example, if a dark photon is produced from stopped pion decay, it can decay into a pair of DM particles (e.g., Refs. [28, 29]). A DM particle would then induce a nuclear recoil event at the detector. The production of a dark photon can occur from both π^0 and the absorption of π^- . The π^0 may produce an ordinary photon and a dark photon which can subsequently decay into two DM particles [29]. However, the π^0 's are not stopped and moving with relativistic speed. In its current configuration, the detectors at the COHERENT experiment are at $\sim 90^\circ$ from the beam direction. The DM arising from the fast-moving π^0 decay lies mostly in the forward direction, so it would thereby miss the detectors. On the other hand, the π^- can create a dark photon via the process, $\pi^- + p \rightarrow n + A'$, followed by the decay of the dark photon A' to a DM pair [28].

The dark photon is emitted isotropically in this π^- absorption process. Further, there can be additional contributions from $\pi^\pm + p/n \rightarrow n/p + \pi^0$, where π^0 's are non-relativistic and again decay to $\gamma + A'$.

The method that we develop to search for DM utilizes both the energy and the timing spectra of the DM-initiated nuclear recoil events. We focus on the timing and energy spectra for the DM produced from the π^- absorption process, since in this case the detector setup at the COHERENT experiment can access the dark photon emerging isotropically from this process. In the COHERENT experiment, the π^- (π^+) abundance per proton on target is 0.05 (0.08) [28, 30]. The dark photon produced from this absorption is mostly relativistic unless the dark photon mass is ~ 138 MeV.

We show that the timing and energy spectra of the DM-nucleus scattering are different from those associated with the neutrino-nucleus scattering. We then develop timing and energy cuts to remove the neutrino background to extract the DM signal. Finally, we apply our analysis technique to the available COHERENT data. We also compare the reach for DM mixing parameter for current and future COHERENT experiments with the projected limit from LDMX and DUNE.

II. DARK MATTER TIMING AND ENERGY SPECTRA

We first derive the timing spectrum of DM-induced nuclear recoil events, followed by a discussion of their energy distribution, and then compare the DM case to that of SM neutrinos. The signal under consideration is initiated by production of a dark photon A' from the decay of the π^-p mesic state through kinetic mixing. A' production and its subsequent decay to DM χ are governed by the following interaction Lagrangian:

$$\mathcal{L}_{\text{int}} \supset g_\chi A'_\mu \bar{\chi} \gamma^\mu \chi + e\epsilon_q A'_\mu \bar{q} \gamma^\mu q, \quad (1)$$

where g_χ and ϵ_q are dark-sector gauge coupling and kinetic mixing parameter, respectively. This generic-looking Lagrangian can be accommodated in the context of a model in e.g., [8, 28].

Suppose that A' is produced at t_F . Since the formation of the mesic state and its decay proceed promptly, t_F is essentially the timing of π^- production induced by the SNS beam. We then assume that A' flies for $v_{A'}(t - t_F)$, in the θ direction of the line joining the Hg

target and the detector, and decays to a χ pair. Since the mesic state is produced nearly at rest, the energy of A' is given by its rest-frame value

$$E_{A'} = \frac{(m_\pi + m_p)^2 - m_n^2 + m_{A'}^2}{2(m_\pi + m_p)}, \quad (2)$$

where m_i denotes the mass of particle species i . One of the χ 's then may travel towards the detector for $v_\chi t'$. Denoting the timing measured at the detector by T , we see that T is the sum of t and t' , i.e., $T = t + t'(v_{A'}(t - t_F), t - t_F, \cos \theta)$, where we explicitly express t' as a function of $t - t_F$ and $\cos \theta$. We are interested in the differential number of events in T , or equivalently the DM flux at the detector of interest, $f(T) = dN_\chi/dT$.

Assuming isotropic emission of A' from the mesic state, we find

$$\frac{d^2 N_{A'}}{dt d \cos \theta} = \frac{1}{2} \cdot \frac{1}{\tau_{A'}} e^{-\frac{t-t_F}{\tau_{A'}}} \Theta(t - t_F), \quad (3)$$

where $\Theta(x)$ is the Heaviside step function. Now a simple change of variable allows us to obtain

$$f(T) \propto \int d \cos \theta \left| \frac{dT}{dt} \right|^{-1} \frac{d^2 N_{A'}}{dt d \cos \theta}. \quad (4)$$

A simple geometry consideration gives $T = t + v_\chi^{-1} \sqrt{x_0^2 + v_{A'}^2 (t - t_F)^2 - 2x_0 v_{A'} (t - t_F) \cos \theta}$ with x_0 being the distance between the Hg target and the detector. One should notice that not all χ particles contribute to $f(T)$ but the ones traveling in the θ' direction do, with θ' measured from the A' moving direction. In other words, the final $f(T)$ needs to be weighted by the relevant probability $w(\cos \theta')$. Labeling the quantities measured in the A' rest frame by an asterisk, we express the weight factor as

$$w(\cos \theta') = \frac{1}{2\pi(v_\chi t')^2} \left| \frac{d \cos \theta'}{d \cos \theta^*} \right|^{-1} \frac{dN_{A' \rightarrow \chi}}{d \cos \theta^*}, \quad (5)$$

where $1/(v_\chi t')^2$ takes care of the flux reduction by the distance between the A' decay point and the detector. Note that $dN_{A' \rightarrow \chi}/d \cos \theta^* = 1$ since each A' decays to two χ 's. Finally, if π^- production timing (proportional to protons on target) is modeled by \mathcal{F} , we obtain

$$f(T) = \int_{-1}^1 d \cos \theta \int_0^{t_F^{\max}} dt_F \left| \frac{dT}{dt} \right|^{-1} \frac{d^2 N_{A'}}{dt d \cos \theta} \cdot w(\cos \theta') \cdot \mathcal{F}(t_F). \quad (6)$$

The left panel of figure 1 demonstrates example timing spectra for a CsI detector, with three different choices for the rest-frame mean lifetime of A' . The solid and dashed histograms are for a relativistic dark photon ($m_{A'} = 75$ MeV) and a non-relativistic dark

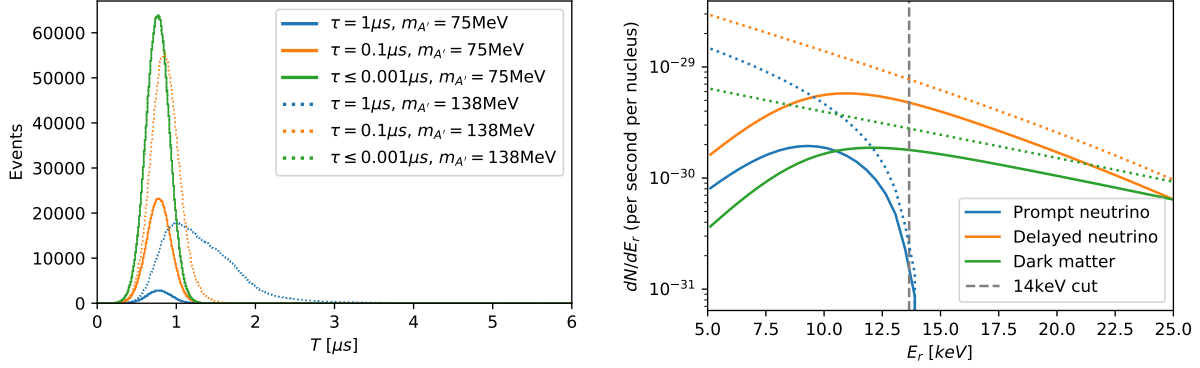


FIG. 1: Left: Timing spectra of DM signal with three different values for $\tau_{A'}$, in a relativistic A' scenario (solid) and a non-relativistic A' scenario (dashed). Right: Nuclear recoil spectrum produced from neutrino and dark matter interactions with (solid) and without (dashed) experimental efficiencies. The vertical dashed line indicates the energy cut that is used to eliminate prompt ν -induced events.

photon ($m_{A'} = 138$ MeV), respectively, with m_χ fixed to 5 MeV. Here the flux \mathcal{F} is approximated by a Gaussian distribution with a mean value of $0.7 \mu\text{s}$ and a width of $0.15 \mu\text{s}$. For the non-relativistic case, most of the χ 's can reach the detector (modulo a factor of $(4\pi x_0^2)^{-1}$). Not surprisingly, as A' is shorter-lived, the spectrum width gets narrower, manifesting in a resonance-like bump feature more visibly. By contrast, for the relativistic case, if A' is long-lived, it decays far away from the detector so that only a small fraction of the χ 's can reach the detector, contributing to the upper tail of the spectrum. Therefore, relatively short-lived A' would give more statistics. Indeed, we see that most of DM events populate within $\sim 1.5 \mu\text{s}$ which roughly corresponds to the mean value plus the width of the beam pulse. Note that prompt neutrinos leave events within $\sim 1.5 \mu\text{s}$ whereas delayed neutrinos spread out over a broad range [9, 30]. So, requiring $T \lesssim 1.5 \mu\text{s}$ essentially rejects most of delayed neutrino events while a large portion of prompt neutrino events and relativistic (non-relativistic) A' -induced DM events irrespective of $\tau_{A'}$ (with $\tau_{A'} \lesssim 0.1 \mu\text{s}$) are kept.

Regarding DM-nucleus scattering, we remark that in principle DM scattering can be governed by physics different from that for dark photon production encoded in Eq. (1). Introducing a generic mediator of mass M' , DM-mediator coupling g_D , and quark-mediator coupling $e\epsilon_q$, we find that the differential spectrum in recoil energy E_r of the target nucleus

can be expressed as

$$\frac{d\sigma}{dE_r} = \frac{e^2 \epsilon_q^2 g_D^2 Z^2 \cdot |F(2m_N E_r)|^2}{4\pi p_\chi^2 (2m_N E_r + M'^2)^2} \left\{ 2E_\chi^2 m_N \left(1 - \frac{E_r}{E_\chi} - \frac{m_N E_r}{2E_\chi^2} \right) + E_r^2 m_N \right\}, \quad (7)$$

where F denotes the form factor and where Z and m_N are the atomic number and the mass of the target nucleus. The underlying interaction is of dark-photon type for illustration. We neglected m_χ in the curly brackets as $m_N \gg m_\chi$. Clearly, the spectral behavior is (nearly) independent of m_χ . The right panel of figure 1 displays the expected nuclear recoil spectrum for $(M', m_\chi) = (75, 5)$ MeV (green). For comparison we show the E_r distributions of the prompt neutrinos (blue) and the delayed neutrinos (orange) with (solid) and without (dashed) experimental efficiencies. We see that prompt neutrino events occur almost entirely in the region $E_r \lesssim 14$ keV, so employing a lower cut at this energy removes the remaining prompt neutrinos, while retaining a large portion of the DM events.

III. APPLICATION TO THE COHERENT DATA

In order to analyze the COHERENT data using both the energy and timing spectra from neutrinos and DM, we adopt the statistical method described in Ref. [27]. We allow for poisson fluctuations of the background in each energy and time bin (model (c) of Ref. [27]), and fix the size of the neutron distribution to $R_n = 4.7$ fm. We also quote our results for $R_n = 5.5$ fm which is the model independent central value obtained from the fit to the COHERENT data [31]. We examine two limiting cases of the data: i) the specific part of the energy and timing data in which the DM signal is predicted to appear, after removing as many neutrino-induced events as possible, and ii) the full energy and timing data set published by COHERENT.

As discussed in the previous section, we apply cuts $E_r > 14$ keV and $T < 1.5 \mu\text{s}$ to substantially suppress both prompt and delayed neutrino events, but keep the DM events¹ for the published COHERENT data. We also apply an upper-cut $E_r > 28$ keV. After these cuts, we find 97 total events. Out of them 49 events have been classified as the steady-state (SS) background, while 19 may be identified as delayed neutrino events forming the SM (i.e., neutrino) background. There are also 3 events

¹ Unless $m_{A'} \approx 138$ MeV and $\tau_{A'} \gtrsim 0.03 \mu\text{s}$.

in the cut window arising from beam related neutron (BRN) backgrounds. There is then an “excess” of 26 events which corresponds to a 2.4σ statistical uncertainty. For $R_n = 5.5$ fm, the significance becomes $\sim 3\sigma$. For calculating the significance we apply $\text{Excess} = (\text{signal} - \text{SS} - \text{BRN} - \text{SM}(\text{neutrino}))/\sqrt{2\text{SS} + \text{BRN} + \text{SM}(\text{neutrino})}$ [32]. We also calculate the significance from the likelihood ratio test for the DM fit to the excess and find the significance to be 1.98.

We first attempt to explain the excess with a DM hypothesis, again assuming that the DM scattering is governed by a different mediator. We fit the selected events, varying the associated (effective) coupling constant ϵ and mediator mass M' which is responsible for the interaction between the DM and the nucleus. The left panel of figure 2 shows 1σ -best fits to the data set with the cuts implemented (blue band). For comparison, the orange band shows the parameter space when performing a fit to the full energy and timing data at 1σ . We see that there exists an overlapping region, and further find that both “before-cut” and “after-cut” data sets are well accommodated by the parameter points with $M' \gtrsim 100$ MeV. For comparison to the DM case, we determine whether a NSI neutrino hypothesis is able to fit both the before-cut and after-cut data. For the neutrino case we consider a non-zero coupling g_e , the NSI in the ν_e neutral-current interaction. As shown in the right panel of figure 2, it is not possible to simultaneously fit both the before-cut and after-cut data sets with this neutrino hypothesis. In fact, this NSI model does not show a good fit for the excess in the prompt timing bin (i.e., $T < 1.5 \mu\text{s}$). The fuzzy region at low g_e shows at there is some statistical consistency with the SM in this region, in particular for the before-cut data. The situation becomes even worse with $g_\mu \neq 0$, since it affects not only the delayed but also the prompt spectrum.

In the DM case, the coupling ϵ is defined as $\epsilon = \epsilon_1^q \epsilon_2^q \epsilon_D \sqrt{\text{BR}_{A' \rightarrow \chi\chi}}$, where ϵ_1^q is the q - A' coupling which describes the dark photon production from the π^- absorption, ϵ_2^q is the quark-mediator coupling for the DM-nucleus scattering cross-section, and $g_D = e\epsilon_D$ is the DM-mediator coupling. This is the most general description, since in a realistic model there can be more than one mediator, e.g., scalar and gauge boson mediators commonly occur in models with spontaneous symmetry breaking. Of course, the best-fit contour can also be interpreted in the case where there exists only a single mediator, i.e., $M' = m_{A'}$.

The parameter choices that we use to obtain the best-fit points are $\tau_{A'} = 1$ ns, $m_{A'} = 75$ MeV and $m_\chi = 5$ MeV. However, we find that the best-fit points do not change in the

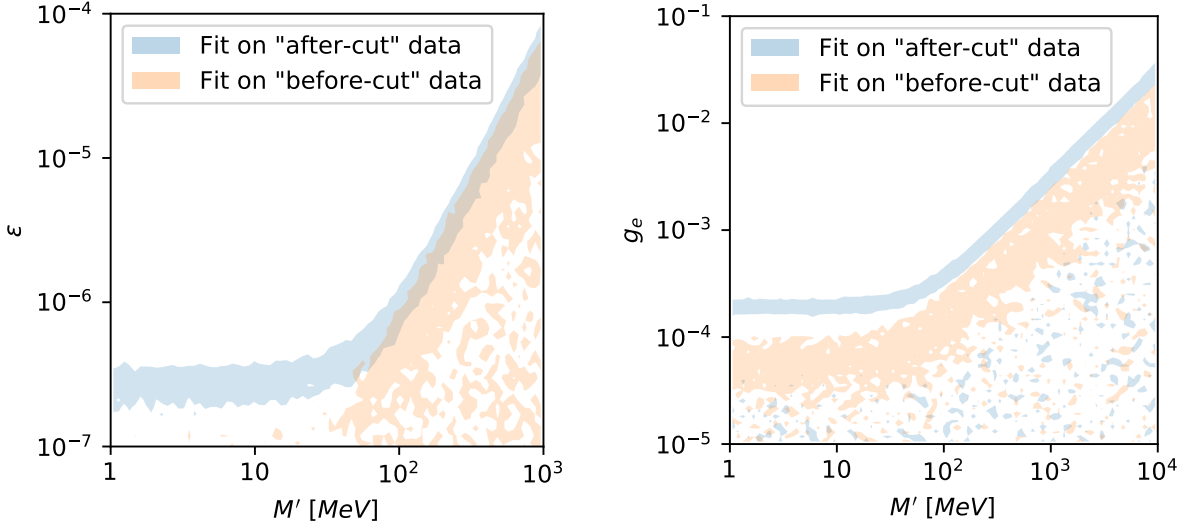


FIG. 2: 1σ best fits to the “before-cut” data (orange) and the “after-cut” data (blue) for a DM interpretation (left panel) and a neutrino NSI interpretation (right panel).

$\epsilon - M'$ plane for the following variations:

- for $\tau_{A'} \lesssim 4$ ns, since the DM flux maximizes for $\tau_{A'} \lesssim 4$ ns with $m_{A'} < 138$ MeV,
- for the non-relativistic case, i.e., $m_{A'} = 138$ MeV, with $\tau_{A'} \lesssim 30$ ns and
- for any m_χ smaller than $m_{A'}/2$.

For relativistic scenarios with large $\tau_{A'}$ (≥ 4 ns), the best-fit regions get scaled by the appropriate associated DM flux (see the left panel of figure 1). For non-relativistic scenarios with large $\tau_{A'}$ (≥ 30 ns), it is not possible to fit before-cut and after-cut data sets simultaneously because DM will contribute to both before $1\mu s$ and after $1\mu s$ events. Figure 2 is shown for $R_n = 4.7$ fm. However, the best fit contours do not change for $R_n = 5.5$ fm.

Based on the above discussions, we describe the best-fit parameters for the following two scenarios.

- Single mediator scenario: In this case, the dark photon A' should decay fast. Otherwise, ϵ needs to be small, meaning that the DM-nucleus scattering is so small that a very small number of events would occur. Here $\epsilon = \epsilon_1^q \epsilon_2^q \epsilon_D \sqrt{\text{BR}_{A' \rightarrow \chi\chi}} \rightarrow (\epsilon^q)^2 \epsilon_D \sqrt{\text{BR}_{A' \rightarrow \chi\chi}}$. We can choose $\epsilon_D = 1/e$ to make $g_D = 1$ which makes $\tau_{A'}$ small,

and we can still make use of the left panel of figure 2 (where $\tau_{A'}$ is set to be ≤ 1 ns) Table I shows the best ϵ^q for a few $M' (= m_{A'})$ values. We do not report any numbers below $M' = 50$ MeV as we find that the best-fit regions with the before-cut data does not overlap with that with the after-cut data.

$M'(\text{MeV})$	50	75	100	1000
ϵ^q	3.5×10^{-4}	4.4×10^{-4}	5.5×10^{-4}	4.6×10^{-3}

TABLE I: Best-fit ϵ^q for a few M' values for the single-mediator scenario.

- Multi-mediator scenario: Unlike the previous scenario, $\tau_{A'}$ is not necessarily small, since χ scatters off the target nucleus via a new mediator with large coupling ($g_D \sim 1$) while the dark photon can decay to the pair of DM particles with a longer lifetime. Table I for a single mediator scenario still holds with $\epsilon^q = \sqrt{\epsilon_1^q \epsilon_2^q}$. Here, ϵ_1^q and ϵ_2^q characterize the dark photon coupling to quarks and DM respectively.

The values of ϵ^q shown in Table I are obtained assuming that the dark photon couplings to up and down quarks are proportional to their charges. If, however, we want to use the universal coupling (e.g., 1), then we need to scale the ϵ^q by $2Z/(9A)$ where $Z = 54$ and $A = 130$ for CsI. The best-fit values of ϵ^q are below any existing bounds [33, 34] arising from meson decays, e.g., $K \rightarrow \pi + \text{invisibles}$. The model details become important for this constraint, i.e., whether it contains fully conserved current, additional Higgs sector [35] and the value of g_D , etc. The COHERENT limit for NSI of neutrinos is better than any existing limit from various experiments using the timing plus energy data where the SM backgrounds cannot be sufficiently suppressed [27]. However, for the DM analysis, since we have vetoed the SM neutrino backgrounds using the energy and timing cuts, we can obtain an even better reach in terms of new physics coupling. If we ignore the excess that we report here after applying the timing and energy cut, the values of ϵ that we find as constraints are only smaller by a factor of 4 compared to the numbers shown in the Table I.

The future LDMX experiment [36] will investigate the sub-GeV DM parameter space which arises from a dark photon decaying to DM, using an electron beam dump. We note that this parameter space is already being probed via nuclear recoils at COHERENT, therefore representing a complementary approach. In figure 3, we compare the reach of ϵ^2 as a function of mediator mass for the current COHERENT data (assuming no excess)

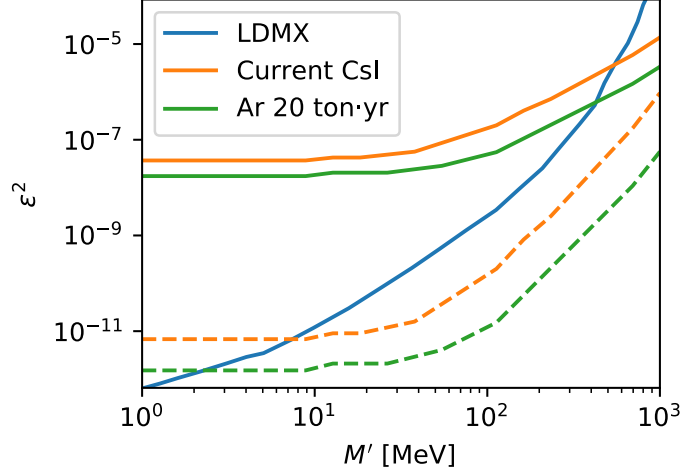


FIG. 3: The coupling ϵ^2 for mediator-nucleus coupling (ϵ_2^g) is shown as a function of M' . The dark photon coupling to the pion absorption (ϵ_1^g) process is the same as ϵ_2^g (solid lines) and is fixed at 10^{-2} (dashed lines).

and for a future Argon detector with the LDMX reach. Our current and projected limits are derived using the formalism of Ref. [21]. We show two scenarios: (i) the dark photon coupling (ϵ_1^g) is the same as the mediator-nucleus coupling (ϵ_2^g) and (ii) ϵ_1^g is fixed at 10^{-2} (current experimental constraint) with $\alpha_D \equiv g_D^2/(4\pi) = 0.5$. We use a dark photon mass $m_{A'} = 75$ MeV and a DM mass $m_\chi = 5$ MeV. The figure, however, is unchanged for $m_{A'} \leq 138$ MeV, $m_\chi \leq m_{A'}/2$ and $\tau_{A'} \leq 4$ ns. We also note that the reach of the current COHERENT data in probing ϵ^2 in figure 3 is better than DUNE experiment reach [37].

IV. CONCLUSIONS

We have argued that the timing information available in neutrino experiments such as the COHERENT data is a powerful probe of new physics. We have shown that the combination of energy and timing cuts can eliminate SM neutrino events very efficiently, thereby allowing the possibility of isolating dark-matter-induced events. As applied to the published COHERENT data, we find a considerable number of excess events over the expected backgrounds. This excess of events may be explained by a dark matter hypothesis, and is unlikely to be explained by SM neutrino interactions. We note that this conclusion is distinct from the results presented in Ref. [27], who showed that using the full energy and timing data without using the cuts, a neutrino model is able to explain the data.

Even though we have presented a dark matter interpretation of the COHERENT data, it remains possible that the events may be explained by an unidentified background, by a systematic uncertainty on the observed steady-state background or by exotic beyond the SM scenarios. Distinguishing a background hypothesis from a dark matter hypothesis may be possible with timing and energy information on individual nuclear recoil events. With this information, an unbinned likelihood analysis may be performed which should allow for a more robust comparison of the spectral shape of the data to the predicted shape of the background, dark matter, and neutrino spectra.

Our analysis strategy can be used to understand dark photon decaying to DM in similar COHERENT type set-ups with timing measurements, e.g. JSNS² [38]. The upcoming data from the ongoing COHERENT and the future runs of the COHERENT and JSNS² experiments would be able to investigate a large region of parameter space in this type of DM models which can be compared with the reach projected by the proposed LDMX and DUNE experiments to probe similar DM scenarios.

ACKNOWLEDGMENTS

We thank Phil Barbeau, Pilar Coloma, Yuri Efremenko, Pedro Machado, Grayson Rich, and Kate Scholberg for useful discussions. BD and LES acknowledge support from DOE Grant de-sc0010813. The work of DK is supported by the Department of Energy under Grant No. DE-FG02-13ER41976/DE-SC0009913. SL acknowledges support from COS-STRP (TAMU). The work of JCP is supported by the National Research Foundation of Korea (NRF-2019R1C1C1005073 and NRF-2018R1A4A1025334). The work of SS is supported by the National Research Foundation of Korea (NRF-2017R1D1A1B03032076 and in partial by NRF2018R1A4A1025334).

-
- [1] E. Aprile et al. (XENON), Phys. Rev. Lett. **121**, 111302 (2018), 1805.12562.
 - [2] M. Battaglieri et al., in *U.S. Cosmic Visions: New Ideas in Dark Matter College Park, MD, USA, March 23-25, 2017* (2017), 1707.04591, URL <http://lss.fnal.gov/archive/2017/conf/fermilab-conf-17-282-ae-ppd-t.pdf>.
 - [3] M. Pospelov, A. Ritz, and M. B. Voloshin, Phys. Lett. **B662**, 53 (2008), 0711.4866.

- [4] D. Hooper and K. M. Zurek, Phys. Rev. **D77**, 087302 (2008), 0801.3686.
- [5] C. Cheung, J. T. Ruderman, L.-T. Wang, and I. Yavin, Phys. Rev. **D80**, 035008 (2009), 0902.3246.
- [6] R. Essig, J. Kaplan, P. Schuster, and N. Toro, Submitted to: Physical Review D (2010), 1004.0691.
- [7] R. Essig et al., in *Proceedings, 2013 Community Summer Study on the Future of U.S. Particle Physics: Snowmass on the Mississippi (CSS2013): Minneapolis, MN, USA, July 29-August 6, 2013* (2013), 1311.0029, URL <http://www.slac.stanford.edu/econf/C1307292/docs/IntensityFrontier/NewLight-17.pdf>.
- [8] B. Dutta, S. Ghosh, and J. Kumar (2019), 1905.02692.
- [9] D. Akimov et al. (COHERENT) (2018), 1803.09183.
- [10] T. Ohlsson, Rept. Prog. Phys. **76**, 044201 (2013), 1209.2710.
- [11] O. G. Miranda and H. Nunokawa, New J. Phys. **17**, 095002 (2015), 1505.06254.
- [12] P. Coloma, P. B. Denton, M. C. Gonzalez-Garcia, M. Maltoni, and T. Schwetz, JHEP **04**, 116 (2017), 1701.04828.
- [13] P. Coloma, M. C. Gonzalez-Garcia, M. Maltoni, and T. Schwetz, Phys. Rev. **D96**, 115007 (2017), 1708.02899.
- [14] J. Liao and D. Marfatia, Phys. Lett. **B775**, 54 (2017), 1708.04255.
- [15] J. B. Dent, B. Dutta, S. Liao, J. L. Newstead, L. E. Strigari, and J. W. Walker, Phys. Rev. **D97**, 035009 (2018), 1711.03521.
- [16] J. Billard, J. Johnston, and B. J. Kavanagh, JCAP **1811**, 016 (2018), 1805.01798.
- [17] M. Lindner, W. Rodejohann, and X.-J. Xu, JHEP **03**, 097 (2017), 1612.04150.
- [18] Y. Farzan, M. Lindner, W. Rodejohann, and X.-J. Xu, JHEP **05**, 066 (2018), 1802.05171.
- [19] V. Brdar, W. Rodejohann, and X.-J. Xu, JHEP **12**, 024 (2018), 1810.03626.
- [20] D. Aristizabal Sierra, V. De Romeri, and N. Rojas, Phys. Rev. **D98**, 075018 (2018), 1806.07424.
- [21] A. Datta, B. Dutta, S. Liao, D. Marfatia, and L. E. Strigari, JHEP **01**, 091 (2019), 1808.02611.
- [22] T. S. Kosmas, D. K. Papoulias, M. Tortola, and J. W. F. Valle, Phys. Rev. **D96**, 063013 (2017), 1703.00054.
- [23] C. Blanco, D. Hooper, and P. Machado (2019), 1901.08094.
- [24] E. Ciuffoli, J. Evslin, Q. Fu, and J. Tang, Phys. Rev. **D97**, 113003 (2018), 1801.02166.

- [25] D. Aristizabal Sierra, J. Liao, and D. Marfatia (2019), 1902.07398.
- [26] D. K. Papoulias, T. S. Kosmas, R. Sahu, V. K. B. Kota, and M. Hota (2019), 1903.03722.
- [27] B. Dutta, S. Liao, S. Sinha, and L. E. Strigari (2019), 1903.10666.
- [28] P. deNiverville, M. Pospelov, and A. Ritz, Phys. Rev. **D92**, 095005 (2015), 1505.07805.
- [29] S.-F. Ge and I. M. Shoemaker, JHEP **11**, 066 (2018), 1710.10889.
- [30] D. Akimov et al. (COHERENT) (2018), 1804.09459.
- [31] M. Cadeddu, C. Giunti, Y. F. Li, and Y. Y. Zhang, Phys. Rev. Lett. **120**, 072501 (2018), 1710.02730.
- [32] K. Scholberg (COHERENT), PoS **NuFact2017**, 020 (2018), 1801.05546.
- [33] R. Essig, J. Mardon, M. Papucci, T. Volansky, and Y.-M. Zhong, JHEP **11**, 167 (2013), 1309.5084.
- [34] J. A. Dror, R. Lasenby, and M. Pospelov, Phys. Rev. **D96**, 075036 (2017), 1707.01503.
- [35] H. Davoudiasl, H.-S. Lee, and W. J. Marciano, Phys. Rev. **D89**, 095006 (2014), 1402.3620.
- [36] T. kesson et al. (LDMX) (2018), 1808.05219.
- [37] V. De Romeri, K. J. Kelly, and P. A. N. Machado (2019), 1903.10505.
- [38] S. Ajimura et al. (2017), 1705.08629.